

Roman situlae from Conimbriga (Portugal): Compositional and microstructural characterization of anthropomorphic handle attachments

Filipa Lopes, Rui J. C. Silva, Maria F. Araújo & Virgílio H. Correia

To cite this article: Filipa Lopes, Rui J. C. Silva, Maria F. Araújo & Virgílio H. Correia (2016): Roman situlae from Conimbriga (Portugal): Compositional and microstructural characterization of anthropomorphic handle attachments, *Materials and Manufacturing Processes*, DOI: [10.1080/10426914.2016.1221102](https://doi.org/10.1080/10426914.2016.1221102)

To link to this article: <http://dx.doi.org/10.1080/10426914.2016.1221102>



Accepted author version posted online: 17 Aug 2016.
Published online: 17 Aug 2016.



Submit your article to this journal [↗](#)



Article views: 34



View related articles [↗](#)



View Crossmark data [↗](#)

Roman *situlae* from *Conimbriga* (Portugal): Compositional and microstructural characterization of anthropomorphic handle attachments

Filipa Lopes^{a,b,c}, Rui J. C. Silva^c, Maria F. Araújo^a, and Virgílio H. Correia^d

^aC2TN, Departamento de Engenharia e Ciências Nucleares, Instituto Superior Técnico, Universidade de Lisboa, Bobadela LRS, Portugal;

^bDepartamento de Conservação e Restauro, Faculdade de Ciências e Tecnologia, Universidade NOVA de Lisboa, Caparica, Portugal; ^c3N/CENIMAT, Departamento de Ciências dos Materiais, Faculdade de Ciências e Tecnologia, Universidade NOVA de Lisboa, Caparica, Portugal; ^dMuseu Monográfico e Ruínas de Conimbriga, Condeixa, Portugal

ABSTRACT

A collection of 33 anthropomorphic handle attachments of Roman *situlae* recovered from the archaeological site of *Conimbriga* (Central Portugal, 2nd century BC–5th century AD) was studied by micro-Energy Dispersive X-Ray Fluorescence Spectrometry (micro-EDXRF), Scanning Electron Microscopy - Energy Dispersive Spectroscopy (SEM-EDS) and metallographic techniques. Regarding the characterization of Roman artifacts of regional production, the relation among typology, composition and microstructure was evaluated in order to infer the Roman influence on the copper metallurgy in Western Iberia. The collection was found to be heterogeneous, mainly constituted by leaded copper and leaded bronzes, with a wide range of lead contents. The artifacts were all produced by mold casting, and most of them show some post-casting processing. Important casting faults and broken artifacts were associated with higher lead contents, and were mainly leaded copper. The leaded bronzes were more carefully produced. The overall results suggest a local metallurgical tradition, with the usage of copper and copper alloy scraps, with high additions of lead. The aim was to produce colored (and cheaper) artifacts, without any major concerns about the finishing details.

ARTICLE HISTORY

Received 16 May 2016
Accepted 28 June 2016

KEYWORDS

Archeological; bronze; copper; *Lusitania*; lead; micro-EDXRF; optical microscopy; SEM-EDS; Western Iberia

Introduction

In the field of Roman metallurgy, everyday implements and local objects are more important to the study of regional traditions in the use of copper alloys than refined, elaborated items, which were often imported [1]. These objects tended to be produced in important industrial centers, and their composition was usually rather standardized [2]. *Situlae* were common artifacts used during the Roman imperial period, originally associated with wine ceremonies with a Bacchic or Dionysiac meaning represented in decorative handle attachments [3]. The taste for such artifacts, diffused all over the Roman provinces, was found in the Iberian Peninsula for a particular metamorphosis, mostly on the handle attachments that tend to evolve along specific regional processes and outlines [3–6]. The Roman city of *Conimbriga* (Central Portugal, 2nd century BC–5th century AD, the site had earlier and later occupations) is an emblematic archeological site in the province of *Lusitania*. Here, large collections of artifacts were recovered during several archeological excavations, even though about 85% of the area of this Roman city still remains unexcavated. Among the many different metallic materials, there is a remarkable collection of anthropomorphic handle attachments of *situlae* (c. 50) [5]. The potential of this collection for the understanding of Roman influence on the metallurgical practices in the western end of the Roman Empire lies in the considerable quantity of material recovered

and the diversity of typologies, some without parallel outside the Iberian Peninsula, with clear evidences of local production. Besides the large amount of metallic artifacts, metallurgical activity remains were also recovered from the excavations. They include tuyeres, tongs, hammers, compasses, chisels, two small crucibles with metal residues [7] and several molds for the manufacture of small-sized objects. Two clay molds were clearly associated with the production of handle attachments (Fig. 2(a)) [8].

In Portugal, in contrast with other regions of the Roman Empire [e.g., 9–16], archeometallurgical studies of Roman materials are scarce, despite the outstanding metallic collections recovered in the Portuguese territory. An earlier investigation on the metallic remains on two crucibles recovered in *Conimbriga* revealed enrichment in Cu, Sn, Zn and Pb on their inner surfaces [7]. Later, the composition of a *patera* handle decorated with a *centaurus* was determined by Energy Dispersive X-Ray Fluorescence Spectrometry (EDXRF) and Synchrotron Radiation X-Ray Fluorescence (SRXRF), and a heavily leaded bronze alloy with a composition similar to those of Roman bronze statues from Eastern Europe was identified [17]. Recently, the analysis of a small set of Roman fibulae and decorated plaques from the archeological site of Castanheiro do Vento (Northern Portugal) determined different types of bronzes alloys – low- and high-tin bronzes, and high-tin leaded

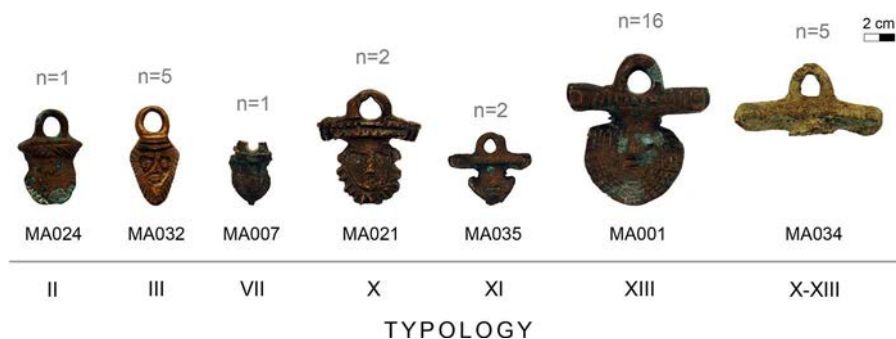


Figure 1. Examples of some of the analysed anthropomorphic handle attachments of *situlae* from *Conimbriga*.

bronzes – evidencing technological and economic choices, indicative of the Roman period [18]. A further recent study of different artifacts from Monte Molião and Cidade das Rosas (Southwestern *Lusitania* province) showed similar variable tin contents (between 2 and 14%) related to the artifacts' function and also high-leaded bronze (19% Pb) used for a decorated handle [19]. Brass and gunmetal alloys were also identified, although only in Cidade das Rosas, a Roman site with a later chronology.

The present study focuses on the elemental and microstructural characterization of 33 selected copper-based handle attachments of *situlae* (Fig. 1). We aim to contribute to a better comprehension of the Roman copper-based metallurgy in the Iberian Peninsula. Micro-EDXRF spectrometry was used to determine the elemental composition of the artifacts, and to ascertain the evolution and compositional patterns of Cu-based alloys. Metallographic examinations by optical microscopy (OM) and complementary Scanning Electron Microscopy - Energy Dispersive Spectroscopy (SEM-EDS) analysis were also performed to characterize their production technology. Observed compositions and microstructures are discussed, by taking into account several typological features of the handle attachments and by comparing the results with those determined on artifacts recovered from other Roman sites.

Materials and methods

The anthropomorphic handle attachments from *Conimbriga* were first studied and classified in four different types according to their features by M. Delgado in 1970 [4]. More recently, a new typological classification of such Roman finds from the Portuguese territory, also based on the shape and decorative features of anthropomorphic handle attachments, but more detailed and establishing 13 different categories, was defined by A. Pinto [5]. In any case, *Conimbriga* was recognized as the major provider of artifacts with diverse typologies. The artifacts selected for this study were classified according to the new categories and identified as types II, III, VII, X, XI, XIII and X-XIII (Fig. 1). Formally, handle attachments consist of three components: escutcheon or face, cross-bar and ring. Some of the selected artifacts could not be assigned to a specific typology, for instance the artifacts classified here as types X-XIII, which were fragmented, without escutcheon, but with a cross-bar that is common from types X-XIII (MA011, MA012, MA031, MA034, MA083). Type XIII presents more dimensional variability, and includes the largest anthropomorphic attachments of the collection, probably coming from larger *situlae*. The majority of the attachments were soldered on the *situlae*. Remnants of the solder were found at the back of some objects (e.g., MA017, Fig. 2(b)). However, there are



Figure 2. a) Bivalve clay mould for the production of anthropomorphic handle attachment of type III found in *Conimbriga*; b) MA017 with remnants of solder at the back; c) MA002 with two rivet holes; d) Casting defects of MA027 with several macropores (black colour); e) MA031 broken artefact with visible cracks; f) Stereo microscope (SM) image of chisel work on MA001; g) MA003 showing wear on ring; h) SM image of MA003 flashing.

two artifacts that were riveted to the *situlae a posteriori*, probably as an alternative join repair (MA002 and MA011, Fig. 2(c)) [3, 4]. This collection is also characterized by the presence of visible casting defects (e.g., macropores and cracks) and some broken artifacts (failures) mainly associated with types XIII and X–XIII. For instance, several open pores cover the surface of artifact MA027 (Fig. 2(d)), while artifact MA035 shows a small fracture at the bottom and reveals large pores. Artifact MA031 is broken and shows many thin parallel cracks on the fracture, visible by the naked eye (Fig. 2(e)).

The handle attachments were first examined under a Zeiss Discovery V20 Stereo Microscope (SM) at up to $7.5\times$ magnification in order to observe macroscopic features (e.g., chisel marks, solder and wear marks), casting defects (e.g., pores, flashing) and cracks.

The elemental composition was determined by micro-EDXRF on five different spots of the small cleaned surface areas, carefully chosen on the back of the handle attachments to minimize the damage and without interfering with their aesthetical value. The analyses were performed using an ArtTAX Pro spectrometer, with a low-power Mo X-ray tube (30 W) and an electro-thermally cooled silicon drift detector with a resolution of 160 eV at 5.9 keV (Mn-K α). The set of polycapillary lens and the accurate positioning system generate a microspot of primary radiation with $\sim 70\ \mu\text{m}$ in diameter [20]. The settings selected for the present analysis were 40 kV of tube voltage, 0.6 mA of current intensity and a live time of 100 s. Quantitative analyses were made with WinAxil software, using the fundamental parameter method and experimental calibration factors that were calculated with certified reference materials: Phosphor Bronze 551 from British Chemical Standards (BCS) and Leaded Bronze C50.01 from the British Non-Ferrous Metals Technology Centre (BNF). Results showed that the standard deviation is less than 5% for major elements, except for Pb (8%). Some larger errors for minor elements are mostly related to strong matrix effects and peak overlapping (particularly Cu and Zn K-lines and As-K α and Pb-L α). The quantification limits for minor elements are: 0.5% for Sn; 0.2% for Zn; 0.1% for Pb and As; 0.07% for Ni and 0.05% for Fe. Additional experimental details were previously published elsewhere [21].

The preparation of the metallic artifacts for OM observations comprises three grinding steps with silicon carbide papers (1000, 2500 and 4000 grits) to clean the corrosion products and reach the bulk metal, and a final polishing using a handheld electric drill equipped with a rotating point of cotton impregnated with diamond paste (from 3 until $1\ \mu\text{m}$ grain size). The micro-EDXRF spectrometry determinations were carried out on the small cleaned areas.

Microstructural examination was conducted in a Leica DMI5000 M OM, coupled to a computer with the LAS V2.6 (Leica M.) and multifocus module software [22], at different magnifications under bright field (BF) illumination.

The microstructural characterization of artifact MA020 was complemented in a scanning electron microscope (SEM) Zeiss model DSM 962 using backscattered electron (BSE) imaging and an energy dispersive spectrometer (EDS) (Oxford Instruments INCAx-sight) with an ultrathin window used for semiquantitative elemental analyses. The experimental conditions were 20 kV of accelerating voltage, approximately

3 A of filament current, $70\ \mu\text{A}$ of emission current and a working distance of 25 mm.

Results and discussion

The results of the elemental analysis and microstructural observations are summarized in Table 1, according to their typologies. Elemental contents determined the Cu-based alloys with Pb and in most cases Sn as major elements, and Zn, Fe, Ni and As frequently present in low amounts. Pb contents are highly variable, with the lowest values of $\sim 2\%$ and reaching $\sim 50\%$. Sn concentrations varied from $<0.5\%$ up to 7.7%. The presence of Zn is rather sporadic, mostly under detection limits, reaching a maximum of 2.7% (MA002). Fe, Ni and As are often present, but in concentrations regularly below 0.5%.

The histogram of distribution of tin (Fig. 3) clearly highlights the existence of two types of alloys: leaded copper and leaded bronzes (Sn $> 2\%$). Sn contents of leaded bronzes follow a Gaussian distribution, with $4.9 \pm 1.6\%$ Sn.

The variable and high amounts of Pb observed in Table 1 can be related to several factors, such as technological, economic or aesthetic [9, 12, 14]. Technologically, the addition of lead to copper alloys was common during the Roman period to improve the castability and cold-workability to allow an easier finishing of ornamental details after casting (e.g., by cold chiseling). Economic factors (Pb was cheaper than other common alloy elements: Sn or Zn) and local availability could also explain the high contents observed. Furthermore, there might have been aesthetic reasons, related to a darker color. High amounts of Pb could be desirable as in Roman metallurgy polychrome effects were intensively exploited (e.g., color contrast with the golden hue of the bronze *situla* body).

The Zn randomly present in low contents (0.1–2.7%) might derive from scrap metal (such as brasses) added to the melt. This would be consistent with the common recycling practices used in Roman times [2, 14, 16]. Some recipes for making bronze statues described in the *Naturalis Historia* refer that *aes collectaneum* (copper-based scrap) was added to the molten metal [23]. Such practices might also explain the low amounts of Sn observed in some of the anthropomorphic attachments.

In order to be able to attribute major variations in composition to possible typological variability, artifacts were grouped according to the different alloys and associated diverse typologies as shown in Fig. 3. The largest group of 19 leaded bronzes collects attachments with several typologies. The group of leaded copper (n = 14) is only associated with types XIII and X–XIII. Artifact MA002, with a somehow distinct composition – a gunmetal with lead, low tin and Zn (3.4% Sn, 2.7% Zn and 19.3% Pb) – belongs to the most common type of figurative attachments (type XIII). Type XI is represented by bronze artifact MA035 and shows the lowest Pb content of the collection (1.8%). Type XIII attachments constitute the majority of artifacts and comprise different alloys.

The values of 5.2 and 6.0% for Sn and 23.2 and 19.0% for Pb, respectively, determined in previously published works on small-sized, decorated castings recovered in Portugal dated to the Roman period, i.e., a *patera* handle with *centaurus* [17]

Table 1. Typological, elemental contents (average values in wt.%; $n=5$) with standard deviation (row below) and microstructural characterization of anthropomorphic attachments from Conimbriga (n.d. – not detected; C – Casting; A – Annealing; W – Mechanical Work; P – Present).

Type	Reference	Chemical composition (wt.%)							Structure		Processing sequence
		Cu	Sn	Pb	Zn	Fe	Ni	As	Cu-S	Phases	
II	MA024*	76.8	5.44	17.8	n.d.	<0.05	n.d.	n.d.	P	(Cu), (Pb), δ	C
		2.8	0.3	2.9							
III	MA020	83.4	2.96	13.0	n.d.	<0.05	0.09	0.53	P	(Cu), (Pb), δ	C
		5.0	1.0	5.7			0.02	0.18			
	MA029	76.8	6.72	16.4	<0.20	0.11	0.08	n.d.	P	(Cu), (Pb), δ	C
		2.9	0.1	2.9		0.15	0.01				
	MA030	82.4	4.51	13.1	n.d.	<0.05	n.d.	n.d.	–	(Cu), (Pb), δ	C + W
		2.6	0.6	3.1							
	MA032	74.2	6.78	19.0	n.d.	0.05	n.d.	n.d.	P	(Cu), (Pb), δ	C + W
2.9		0.2	2.8		0.04						
MA033	83.4	4.08	10.6	n.d.	1.77	n.d.	n.d.	P	(Cu), (Pb), δ	C + W	
	2.0	0.3	2.2		0.32						
MA084	86.7	7.72	5.00	0.29	0.25	n.d.	n.d.	P	(Cu), (Pb), δ	C + W	
	1.9	0.7	2.4	0.02	0.04						
VII	MA007 [†]	78.2	4.44	16.9	<0.20	0.05	0.09	0.12	–	(Cu), (Pb), δ	C + W
		6.3	0.2	6.4		0.03	0.01	0.06			
X	MA021*	87.0	3.56	9.66	n.d.	n.d.	n.d.	n.d.	P	(Cu), (Pb), δ	C + W
		5.9	0.5	6.0							
MA028*	82.3	5.34	12.3	n.d.	0.08	n.d.	n.d.	P	(Cu), (Pb), δ	C + W	
	2.9	0.4	3.0		0.07						
XI	MA022*	81.3	4.26	14.1	n.d.	0.05	0.13	n.d.	P	(Cu), (Pb), δ	C + (W + A) + W
		2.6	0.2	2.7		0.05	0.01				
MA035*	94.3	3.85	1.82	n.d.	<0.05	n.d.	0.21	P	(Cu), (Pb)	C	
	1.9	1.6	0.7				0.06				
XIII	MA001	70.0	5.46	23.5	0.65	0.09	n.d.	0.18	–	(Cu), (Pb), δ	C + (W + A) + W
		8.5	0.6	9.1	0.13	0.01		0.10			
MA002 [‡]	74.3	3.42	19.3	2.66	0.09	0.09	n.d.	–	(Cu), (Pb), δ	C + W	
	14.8	0.5	14.8	0.6	0.01	0.01					
MA003*	80.5	4.72	14.8	n.d.	0.06	n.d.	n.d.	P	(Cu), (Pb)	C + (W + A) + W	
	3.2	0.2	3.2		0.02						
MA004 [†]	93.0	0.72	5.66	0.22	<0.05	n.d.	n.d.	–	(Cu), (Pb)	C	
	2.3	0.3	2.3	0.04							
MA006* [†]	83.6	1.40	14.6	n.d.	<0.05	0.09	0.19	–	(Cu), (Pb), δ	C	
	5.4	1.1	5.0			0.01	0.13				
MA008 [†]	92.2	0.75	6.40	0.29	<0.05	0.18	<0.10	–	(Cu), (Pb)	C + (W + A)	
	5.1	0.0	5.2	0.02		0.01					
MA009 [†]	71.2	0.70	28.0	n.d.	<0.05	0.2	0.15	–	(Cu), (Pb), δ	C	
	3.7	0.7	4.0			0.01	0.09				
MA010 [†]	73.2	1.07	25.6	n.d.	0.08	0.12	0.2	P	(Cu), (Pb)	C + (W + A)	
	3.9	0.2	3.8		0.10	0.02	0.26				
MA016*	88.1	1.93	9.38	0.21	<0.05	0.13	0.18	P	(Cu), (Pb), δ	C	
	6.1	0.1	6.0	0.12		0.02	0.06				
MA017*	82.9	3.30	14.0	n.d.	n.d.	n.d.	n.d.	P	(Cu), (Pb), δ	C	
	4.3	0.7	5.1								
MA018	83.4	2.02	14.4	n.d.	<0.05	n.d.	<0.10	–	(Cu), (Pb)	C + (W + A)	
	5.8	0.7	5.4								
MA019 [†]	90.9	0.95	3.48	0.48	0.08	0.08	0.71	P	(Cu), (Pb)	C	
	6.4	0.3	1.2	0.36	0.10	0.01	0.22				
MA023*	78.0	5.84	16.2	n.d.	<0.05	0.07	n.d.	P	(Cu), (Pb), δ	C + W	
	1.6	0.3	1.9			0.01					
MA025 [†]	74.9	7.76	16.2	0.82	0.19	n.d.	n.d.	P	(Cu), (Pb)	C + W	
	3.0	0.4	2.9	0.16	0.10						
MA026 [†]	82.1	1.88	14.7	1.13	0.21	0.09	n.d.	–	(Cu), (Pb)	C + W	
	5.6	0.1	5.8	0.11	0.17	0.00					
MA027	84.5	1.45	14.2	n.d.	<0.05	n.d.	n.d.	–	(Cu), (Pb), δ	C + (W + A)	
	7.8	0.3	7.4								
X-XIII	MA011 [‡]	72.2	1.52	25.8	n.d.	0.36	0.13	<0.10	P	(Cu), (Pb)	C
		0.9	0.1	1.3		0.06	0.03				
MA012 [†]	79.7	0.68	19.5	n.d.	<0.05	<0.07	<0.10	–	(Cu), (Pb), δ	C	
	5.5	0.1	5.6								
MA031 [†]	50.5	0.55	48.9	n.d.	<0.05	0.11	n.d.	–	(Cu), (Pb)	C	
	4.0	0.4	3.8			0.02					
MA034 [†]	75.7	1.32	22.8	n.d.	0.13	0.07	n.d.	P	(Cu), (Pb)	C	
	2.9	0.0	2.6		0.02	0.01					
MA083 [†]	70.1	<0.50	29.2	n.d.	<0.05	0.1	n.d.	–	(Cu), (Pb), δ	C	
	4.7	0.0	4.6			0.01					

*Remnants of solder.

[†]Broken artifacts.[‡]Riveted.

and the decorated handle of a jug [19], are similar to the ones of leaded bronze handle attachments from *Conimbriga*.

A further publication on three anthropomorphic attachments from Spain, analyzed by Ruano et al. [6], reports

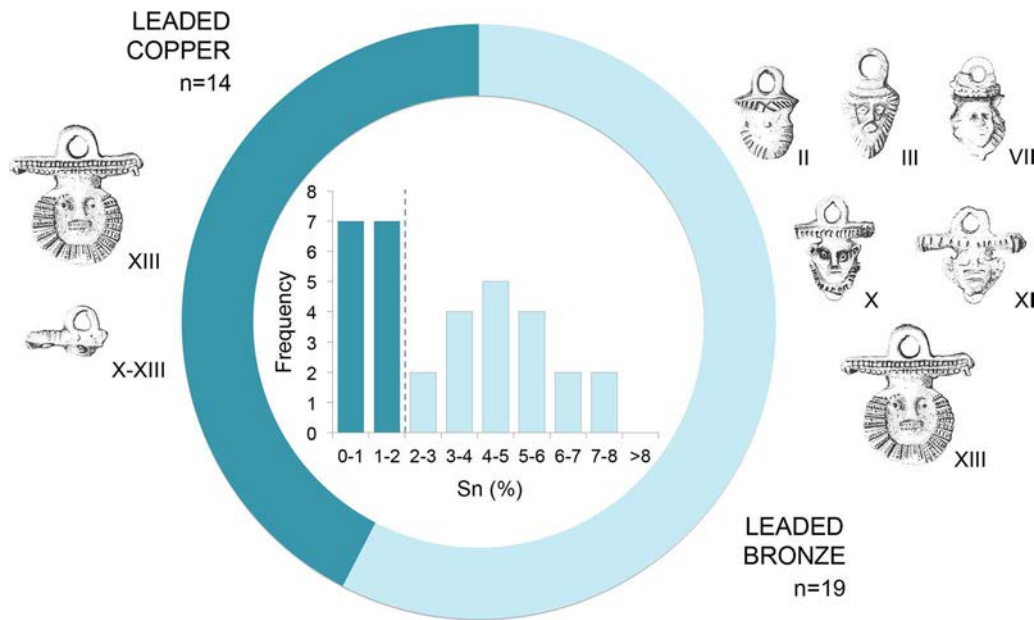


Figure 3. Inside of the image: distribution of tin contents in the anthropomorphic attachments analysed where the dashed line separates led copper from led bronzes; outside: distribution of different typologies of anthropomorphic attachments according to alloy types. Archaeological drawings adapted from Delgado, 1970 [4].

compositions that are similar to those from *Conimbriga*. One of the attachments, corresponding to type XII, has 5.7% Sn and 18.4% Pb, and is identical to MA022 (types XI–XII). The two other attachments corresponding to type XIII, with 2.8 and 2.6% Sn, and 22 and 22.9% Pb, also fit in the picture of *Conimbriga* compositions of led copper-tin alloys of the same typology. On the other hand, two handle attachments of a complete *situla* from the Czech Republic [24], dated to the end of the 1st century BC, contain 9.9 and 10.1% Sn and 8.1 and 3.3% Pb, and show a different compositional pattern. However, these artifacts, representing a female head ornamented with the head of a panther on both sides, show a fine decoration, and are much more elaborated. The Czech attachments might have been produced in the region Campania, in Italy [24], which is considered to be the main center for the production of luxurious bronze vessels for internal consumption and for export during the Roman period [23, 25].

In general, the Pb contents of anthropomorphic attachments from *Conimbriga* are in agreement with the composition of small Roman statuettes, found in France [9], Germany [26] and in the Southern Alps [27], reaching, in some cases, Pb contents of over 30%. They also follow the line of earlier high-lead alloys used for artifacts with similar function but different aesthetics, coming from Greece and Etruria [28]. The main peculiarity in the case of the *Conimbriga* artifacts is the presence of led copper in such elaborated, small and decorative objects that, to our knowledge, has not been reported in other regions. According to Giunlia-Mair [27], in this period and all over the Roman world, the massive substitution of binary bronzes and unalloyed copper occurred with an increasing use of led bronzes, led brasses and quaternary copper alloys with Sn, Zn and Pb.

In general, the composition of led bronze handle attachments of *situlae* is comparable to the general picture of arbitrary compositions from previously published Roman

small castings [9, 26]. It is clear that in *Conimbriga* there was no standard Cu/Pb or Cu/Sn ratio used by smiths to produce the handle attachments of *situlae*, as it is documented for other typologies of Roman artifacts from Italy, which show well-established compositions, such as hammered bronze vessels (10% Sn; Pb < 1%), bells to achieve a specific sound (20% Sn; Pb < 5%) or mirrors to reflect the image ($\geq 20\%$ Sn) [2].

Microstructural features (Table 1) indicate a similar manufacturing process for all handle attachments: shaping by casting in a mold with or without further mechanical operations and/or heat treatments. Three possible combinations of post-casting operations could be identified (Fig. 4(a)):

- C + W: casting (C) plus mechanical work (W), as forging, hammering, polishing, chiseling or cutting – presenting characteristic slip bands in (Cu) grains;
- C + (W + A): casting followed by one or more cycles of mechanical work plus annealing (A) operations – presenting characteristic annealing twins in (Cu) grains;
- C + (W + A) + W: casting followed by one or more cycles of mechanical work plus annealing operations ending with final metal working – presenting both annealing twins and slip bands.

Casting in a mold would be the manufacturing technique expected, since artifacts were identical: small decorative items with a functional purpose. An as-cast (C) condition is observed with a relative frequency in 46% of the artifacts (Fig. 4(a)), associated with the majority of typologies (II, III, XI, XIII and X–XIII) (Fig. 4(b)) for both led copper and led bronze (Table 1). Types X–XIII show an as-cast condition (Fig. 4(b)) – associated with broken artifacts made of led copper with a high lead content (19.5–48.9%) (Table 1). Many of the anthropomorphic attachments are fragmented, in particular types XIII and X–XIII and all are made of led copper (Table 1). A possible explanation can be related to the shape and function of these attachments, which are thinner than others from different typologies and present a cross-bar,

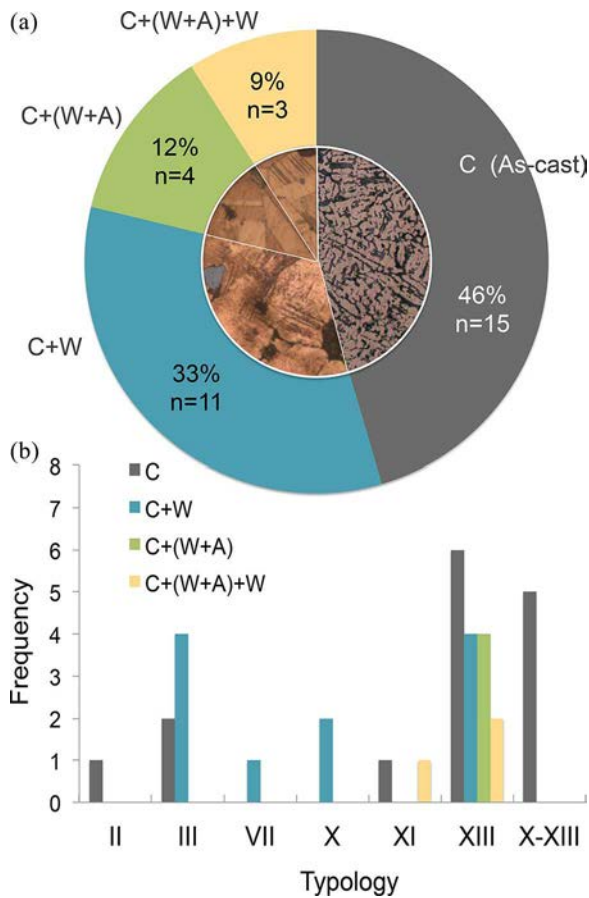


Figure 4. a) Distribution of manufacturing procedures of the 33 anthropomorphic handle attachments observed at OM. b) Distribution of processing sequences by typologies of the anthropomorphic handle attachments ($n = 33$).

similar to types X, XI and XII, although in most cases larger and wider. A high Pb content is disadvantageous for such artifacts, which are subjected to substantial mechanical stress, because the Pb-rich phase weakens the material. Due to the high immiscibility of Pb in (Cu) solid solution, Pb is segregated during the solidification process. According to the Cu–Pb equilibrium phase diagram [29], there is a monotectic reaction at 955°C (forming an immiscible Pb-rich liquid during solidification) and a eutectic reaction at 226°C (the liquid solidifies in a Pb-rich eutectic: 99.9% Pb). For copper alloys with lower Pb contents, the Pb-rich eutectic is present in the globular form in the

final microstructure, because of the high immiscibility of the Pb-rich liquid with the rest of the liquid with a monotectic composition (36% Pb) [30]. On the other hand, for alloys with higher lead contents inter-dendritic shapes are expected, since the proportion of Pb-rich liquid prevails during solidification, filling in the spaces between (Cu) dendrites. In the analyzed collection, relatively large Pb-rich globules were observed in artifacts MA009 and MA012 with 28% and 19.5% Pb, respectively (Fig. 5(a)). This might be explained by the lower cooling rates during solidification [31, 32], with enough time for the Pb-rich liquid droplets to merge (coalescence phenomenon) in larger globules. For the single artifact with a Pb content above 36% (MA031 with 48.9% Pb), an interdendritic Pb-rich structure can be observed (Fig. 5(b)), as expected for high Pb contents.

Most of the thermomechanical-processed features observed are not very pronounced, some annealing twins (slightly recrystallized structure) and a few slip bands over a cored (Cu) dendritic structure (typical feature in as-cast structure) are visible, with the common presence of (Pb), δ -Cu, Sn phase and Cu-S inclusions. This means that the thermomechanical sequences should be considered mainly as a surface finishing process on the as-cast shape. The δ phase is generally found in cast bronzes with more than 6–8% Sn and also in an experimental water-quenched bronze with 2% Sn [33]. In the majority of handle attachments observed at OM, this Sn-rich phase (with a light grey color in BF) was found in leaded bronzes and leaded copper, in some cases with less than 1% Sn (Table 1). This behavior can be explained by taking into account the effect of Pb in ternary Cu–Pb–Sn alloys (see Fig. 5: Cu–Pb–Sn, Isothermal section at 400°C [34]), where the increase of Pb contents renders the Sn solubility in (Cu) solid solution, and promotes the δ phase.

Different phases and inclusions observed in OM were clearly identified by SEM-EDS analysis (Fig. 6). The OM observations also revealed the existence of deep interdendritic corrosion in some of the “cleaned” areas, as a result of the preferential oxidation of Pb and Sn (de-alloying corrosion). In the case of Pb, this process might result in an important leaching of this element, mostly concentrated in the Pb-rich eutectic. For the Sn present in the (Cu) solid solution, but especially in the δ phase, the oxidation process might produce a copper redeposition, a kinetically slow mechanism that occurs under certain burial conditions at low-oxygen potential [35, 36], as it was observed in the microstructure of the artifact

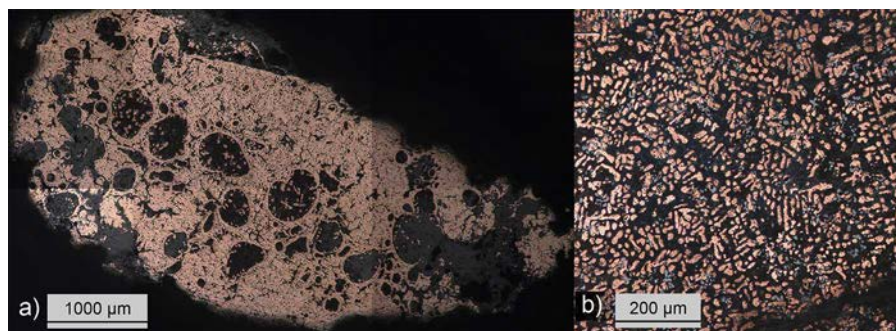


Figure 5. a) Microstructure of handle attachment MA012 exhibiting large globules of Pb-rich eutectic in a (Cu) and interdendritic (Pb) matrix (OM; BF). b) High leaded copper microstructure of handle attachment MA031 showing interdendritic Pb-rich eutectic with a crack (OM; BF; etched).

MA020 (Fig. 6). Bosi et al. [35] classified the unalloyed copper inclusions (UCIs) of metallic copper into three types. The observed morphologies on MA020 (Fig. 6) seem to fit in type A –“irregularly shaped UCI, that pseudomorphically replace other phases” [35] – but in the present case, they are surrounded by a Sn–Pb–O-rich layer. The presence of these UCIs might be explained by the fact that low-oxygen potentials in deeper intergranular corrosion regions are not sufficient to oxidize the more noble elements, such as Cu. The consequence of these corrosion processes is that the current evaluation of Sn and Pb contents in these artifacts by micro-EDXRF must be lower than originally. However,

because of the high insolubility of the major corrosion product of Sn (Sn_2O), this element has a less-significant loss than Pb.

Type III comprises two types of microstructural features: as-cast and cast plus final hammering, associated with leaded bronzes (Fig. 3(a)). The flashing was removed in most of the cold-worked attachments.

Among the studied artifacts presenting additional operations after casting, 33% showed C + W processing, 12% were subjected to C + (W + A) operation cycles and only three artifacts (9%) showed a C + (W + A) + W operational sequence (Fig. 4). This last group comprises MA001, MA003 and MA022 (leaded bronzes) and belongs to types XI and XIII.

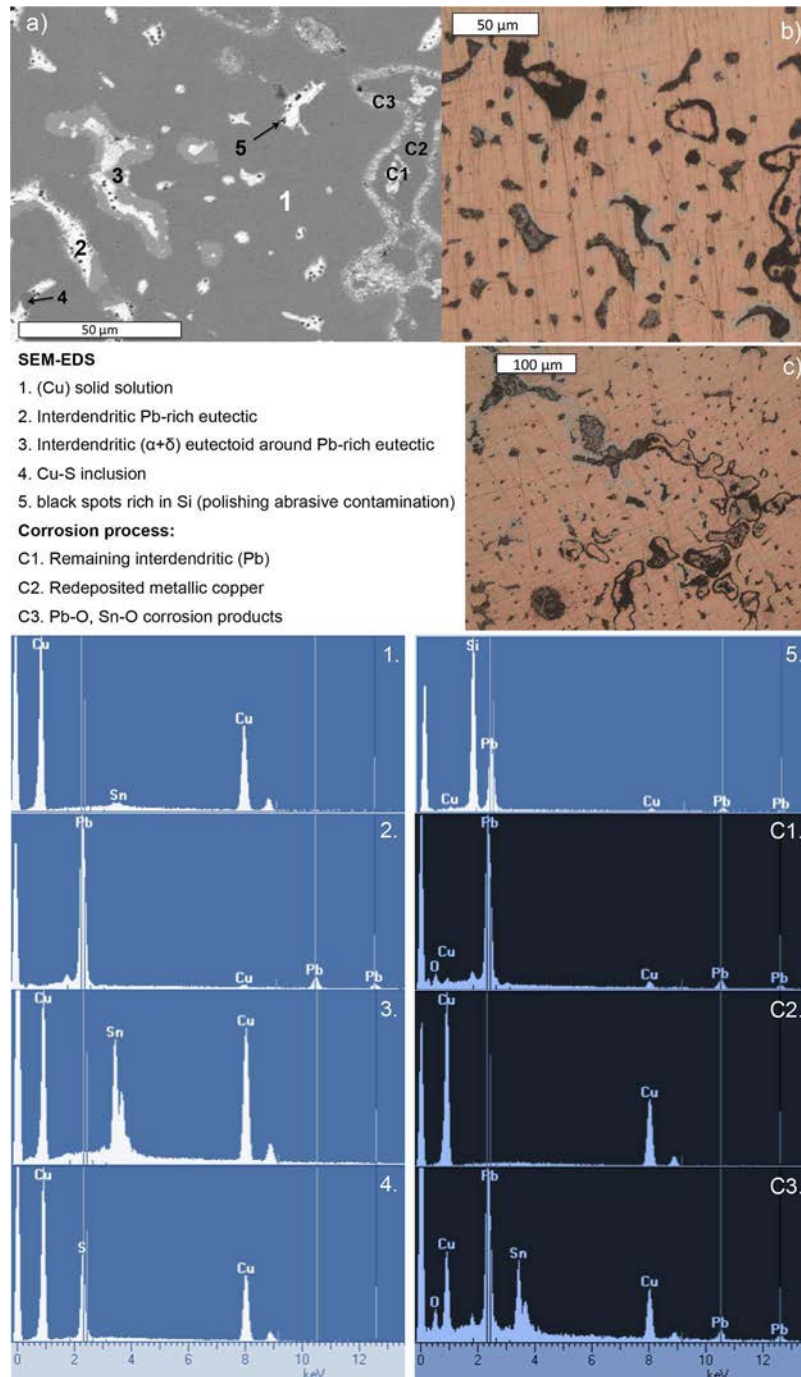


Figure 6. Microstructure of anthropomorphic handle attachment MA020: a) SEM image with several points of analysis by EDS related to original microstructure (1-5) and corrosion process (C1-C3); b) OM image of the area analysed by SEM (BF); c) OM general view (BF).

Apparently the smiths made an extra effort in their manufacture, even though the objects are aesthetically far from their more luxurious imperial counterparts. Additionally, MA001 shows another detail in the finishing of the face: cold work with chisel (Fig. 2(f)). The high Pb content (23.5% average content) facilitates a final chiseling.

Type XI is represented by MA022, an intensively worked artifact, and MA035, left in as-cast condition (Fig. 4(b)). MA022 also shows wear marks in the ring and the remnants of the solder. However, flashing was not removed during the finishing processes. There are other artifacts presenting flashing with clear evidences of use (e.g., MA003, MA020, MA035) (Fig. 2(g), (h)), independent of their thermomechanical treatment after casting and suggesting that finishing was not always a concern for the metalworker. Solder remains were found at the back of 11 handle attachments (see Table 1). They are easily identified by their characteristic silvery color, due to the high Sn contents in Cu–Sn solders (MA017, Fig. 2(b)). Preliminary results by SEM-EDS analysis found average values of 35% Sn. The handle attachments with solder remains were compared to check whether the soldering process could be associated with a particular manufacturing sequence, but no correlation was observed.

Artifacts from type XIII are mainly in as-cast condition and are predominantly leaded copper. Nevertheless, besides being the most numerous typology ($n = 16$), this group presents a wider diversity in additional thermomechanical operations after casting, usually in the case of leaded bronzes (Fig. 4(b)). This fact could be explained by the characteristic shape of the artifacts, which show a large cross-bar requiring additional work (plastic deformation) to fit in the rim of the *situla*.

Conclusions

The 33 anthropomorphic handle attachments studied for this research are all copper-based alloys: leaded copper and leaded bronzes, with a common presence of high amounts of lead. The shape of the handle attachments was obtained by mold casting and the majority of the artifacts were subjected to mechanical work and/or annealing operations after casting. A tendency for leaded bronzes to be subjected to finishing operations was observed. However, finishing and cold work were not a general practice (except for type III). This was shown by the presence of flashing in artifacts that were undoubtedly used. Type XIII revealed the largest variability of the *chain opératoire* and elemental composition, being also the most representative typology found in *Conimbriga*.

The variability and compositional patterns of copper alloys with low Sn and high Pb also evidenced that this collection consists of inexpensive metallurgical production, and does not show the high quality we are used to in the Roman metallurgical scenario.

Quantity, variety of typologies (with some unique characteristics), variety of alloys, recycling, high lead contents (cheaper alloys), easily reproduced small-size castings, casting defects (low-quality, broken artifacts) and unfinished surfaces (with evidences of usage) are all valid indications of low-quality metalwork.

Funding

This work was funded by FEDER funds through the COMPETE 2020 Programme and National Funds through FCT (Portuguese Foundation for Science and Technology), under project number POCI-01-0145-FEDER-007688, Reference UID/CTM/50025/2013 to i3N/CENIMAT and the project UID/Multi/04349/2013 to C²TN/IST. The PhD grant SFRH/BD/85329/2012 by FCT to FL is also acknowledged.

References

- [1] Giunilia-Mair, A. Roman metallurgy: Workshops, alloys, techniques and open questions; In *Proceedings of the International Conference on Ancient Metallurgy between Oriental Alps and Pannonia Plain Workshop*, Trieste, Italy, Oct. 29–30, 1998. Quaderni dell'Associazione Nazionale per Aquileia, vol. 8, Trieste, 2000; 107–120.
- [2] Riederer, J. The use of standardised copper alloys in Roman metal technology. In *I bronzi antichi: produzione e tecnologia*. Atti del XV Congresso Internazionale sui Bronzi Antichi, Grado-Aquileia, May 22–26, 2001, Giunilia-Mair, A. Ed., Monique Mergoil: Montagnac, 2002; 284–291.
- [3] Lacabe, R.E. La situla de *Caesaraugusta*-Zaragoza y los apliques tipo III de Delgado. *Archivo Español de Arqueología* **2006**, *79*, 271–280.
- [4] Delgado, M. Elementos de situlas de bronce de conimbriga. *Conimbriga* **1970**, *IX*, 15–43.
- [5] Pinto, A. *Bronzes Figurativos Romanos de Portugal*. Fundação Calouste Gulbenkian: Lisboa, 2002.
- [6] Castelo Ruano, R.; Gómez Ramos, P.; Torrecilla Aznar, A.; Arribas Dominguez, R.; Panizo Arias, I. Apliques de asas de situlae con decoración antropomorfa procedentes de la villa romana de El Saucedo (Talavera La Nueva, Toledo). *CuPAUAM* **1995**, *22*, 125–164.
- [7] Cabral, J.M.P.; Araújo, M.F.; Alarcão, A.M. Análise química não-destrutiva de dois cadinhos achados em Conimbriga. *Conimbriga* **1983**, *XXIII*, 159–168.
- [8] Alarcão, J.; Etienne, R.; Alarcão, A.M.; Ponte, S. *Fouilles de Conimbriga VII, Trouvailles Diverses, Conclusions Générales*. De Boccard: Paris, 1979.
- [9] Picon, M.; Condamine, J.; Boucher, S. Recherches techniques sur des bronzes de Gaule romaine, I. *Gallia* **1966**, *24*, 189–215. doi:10.3406/galia.1973.2628.
- [10] Picon, M.; Condamine, J.; Boucher, S. Recherches techniques sur des bronzes de Gaule romaine, II. *Gallia* **1967**, *25*, 153–168. doi:10.3406/galia.1973.2628.
- [11] Picon, M., Condamine, J., Boucher, S. Recherches techniques sur des bronzes de Gaule romaine, III. *Gallia* **1968**, *26*, 245–278. doi:10.3406/galia.1973.2628.
- [12] Craddock, P. Copper alloys of the Hellenistic and Roman world: New analyses and old authors. In *Aspects of Ancient Mining and Metallurgy. Acta of a British School at Athens Centenary Conference*, 1986, 55–65. Jones J.E. Ed.; Bangor: University College of Wales, 1988.
- [13] Unglik, H. Structure, composition, and technology of Late Roman copper alloy artifacts from the Canadian excavations at Carthage. *Archaeomaterials* **1991**, *5*, 91–110.
- [14] Dungworth, D. Roman copper alloys: Analysis of artefacts from Northern Britain. *Journal of Archaeological Science* **1997**, *24* (10), 901–910.
- [15] Bayley, J.; Butcher, S. *Roman brooches in Britain: A technological and typological study based on the Richborough collection*; Society of Antiquaries of London: London, 2004.
- [16] Fácşády, A.R.; Verebes, A. Analysis of Roman bronze finger rings from Aquincum. *Materials and Manufacturing Processes* **2009**, *24* (9), 993–998. doi:10.1080/10426910902979942.
- [17] Araújo, M.F.; Pinheiro, T.; Valério, P.; Barreiros, A.; Simionovici, A.; Bohic, S.; Melo, A. Analysis of a Roman *Centaurus* from Canas de Senhorim (Portugal): Comparative study using EDXRF and SXRF. *Journal de Physique* **2003**, *IV* (104), 523–526. doi:10.1051/jp4:20030137.

- [18] Valério, P.; Araújo, M.F.; Silva, R.J.C. Complementary use of X-ray methods to study ancient production remains and metals from Northern Portugal. *X-Ray Spectrometry* **2014**, *43* (4), 209–215. doi:10.1002/xrs.2541.
- [19] Valério, P.; Voráčová, E.; Silva, R.J.C.; Araújo, M.F.; Soares, A.M.M.; Arruda, A.M.; Pereira, C. Composition and microstructure of Roman metallic artefacts of Southwestern Iberian Peninsula. *Applied Physics A* **2015**, *121* (1), 115–122. doi:10.1007/s00339-015-9394-7.
- [20] Bronk, H.; Röhrs, S.; Bjeoumikhov, A. ArtTAX: A new mobile spectrometer for energy-dispersive micro X-ray fluorescence spectrometry on art and archaeological objects. *Fresenius Journal of Analytical Chemistry* **2001**, *371* (3), 307–316. doi:10.1007/s002160100989.
- [21] Valério, P.; Araújo, M.F.; Canha, A. EDXRF and micro-EDXRF studies of Late Bronze Age metallurgical productions from Canedotes (Portugal). *Nuclear Instruments and Methods B* **2007**, *263*, 477–482. doi:10.1016/j.nimb.2007.07.004.
- [22] Figueiredo, E.; Silva, R.J.C.; Araújo, M.F.; Fernandes, F.M.B. Multifocus optical microscopy applied to the study of archaeological metals. *Microscopy and Microanalysis* **2013**, *19* (5), 1248–54. doi:10.1017/S1431927613001608.
- [23] Pliny the Elder, *The Natural History*, John Bostock, M.D., F.R.S., H.T. Riley, Esq., B.A., Eds., Taylor and Francis: London; 1985, Book 34, Chapter 20. Retrieved July 9, 2015, from <http://data.perseus.org/citations/urn:cts:latinLit:phi0978.phi001.perseus-eng1:34.20>.
- [24] Msallamová, Š.; Kmošek, J. Determination of causes of corrosion damage of a roman vessel from an early Tiberian period. *Materials Science Forum* **2014**, *782*, 645–648. doi:10.4028/www.scientific.net/MSF.782.645.
- [25] Tucker, C. Two Roman bronze vessels from St. Nicholas at Wade, Isle of Thanet. *Archaeologia Cantiana* **2012**, *132*, 189–213.
- [26] Riederer, J. Die Berliner Datenbank von Metallobjekten kulturgeschichtlicher Objekte.III. Römische Objekte. *Berliner Beiträge zur Archäometrie* **2001**, *18*, 139–259.
- [27] Giunlia-Mair, A. Copper and copper alloys in the Southeastern Alps: An overview. *Archaeometry* **2005**, *47* (2), 275–292.
- [28] Craddock, P.T. The composition of the copper alloys used by the Greek, Etruscan and Roman civilizations 1. The Greeks before the archaic period. *Journal of Archaeological Science* **1976**, *3* (2), 93–113. doi:10.1016/0305-4403(76)90079-0.
- [29] Lyman, T., *Metals Handbook, Volume 8: Metallography, Structures and Phase Diagrams*, 8th Edition, American Society for Metals (ASM): Ohio, USA, 1973.
- [30] Campbell, F.C. ed. *Elements of Metallurgy and Engineering Alloys*, ASM International: Ohio, USA, 2008.
- [31] Hughes, M.J.; Northover, J.P.; Staniaszek, B.E.P. Problems in the analysis of leaded bronze alloys in ancient artefacts. *Oxford Journal of Archaeology* **1982**, *1* (3), 359–364. doi:10.1111/j.1468-0092.1982.tb00320.x.
- [32] Martyushev, N. Parameters of the dendritic structure of copper alloys. *Chemistry of Metals and Alloys* **2011**, *3* (2010), 197–200.
- [33] Wang, Q., Ottaway, B. *Casting Experiments and Microstructure of Archaeologically Relevant Bronzes*; Archaeopress (BAR International Series 1331): Oxford, 2004.
- [34] Materials Science International Team MSIT. Non-ferrous metal systems. In *Selected Soldering and Brazing Systems, Part 3. Ternary Alloy Systems - Phase Diagrams, Crystallographic and Thermodynamic Data*, Vol. 11. Landolt-Börnstein - Group IV Physical Chemistry; Effenberg, G.; Ilyenko, S. Eds., Springer: Berlin, Heidelberg, 2007, 1–17. doi:10.1007/978-3-540-47004-5_1.
- [35] Bosi, C.; Garagnani, G.L.; Imbeni, V.; Martini, C.; Mazzeo, R.; Poli, G. Unalloyed copper inclusions in ancient bronze artefacts. *Journal of Materials Science* **2002**, *37*, 4285–4298.
- [36] Quaranta, M.; Catelli, E.; Prati, S.; Scitutto, G.; Mazzeo, R. Chinese archaeological artefacts: Microstructure and corrosion behaviour of high-leaded bronzes. *Journal of Cultural Heritage* **2014**, *15* (3), 283–291. doi:10.1016/j.culher.2013.07.007.